Surface Analysis

DOI: 10.1002/anie.201003335

Mesoscopic Arrays from Supramolecular Self-Assembly**

Sylvain Clair, Mathieu Abel,* and Louis Porte*

Supramolecular chemistry on a surface is a particularly creative way of producing two-dimensional well-ordered networks, as demonstrated by the large number of recent studies.[1–7] Indeed, a self-assembled organic film can act as an organic nanoscale template with a rich variety in size, symmetry, and functionality of the two-dimensional network, which can potentially accommodate guest molecules.[8–12] However, the amplitude of these structures is usually restricted by the size of one molecular precursor (or tecton), which is for practical reasons no more than about 1 or 2 nm. In some cases it is possible to overcome this limitation by taking advantage of a dislocation network of the metal substrate,[13,14] but then the complexity of the system is noticeably enhanced. Examples of large two-dimensional networks self-assembled on homogeneous substrates with a unit cell comprising only one tecton are rare.[15–20] In these examples, the superstructures are formed by kinetic limitation (metastable phase),[15] through indirect registry effects with the substrate,[16,17] or by influence of total molecular coverage.[18–20] In the latter case, high-order superstructures provide a denser packing but are energetically less favored and can be obtained only at increasing surface coverage: the superstructure size is an extensive property of the system. The formation of one-dimensional templates or nanogratings with large (mesoscopic) interline distances has also been reported, but again the periodicity was directly related to the molecular coverage.[21–23] Herein we present an exceptionally large two-dimensional organic template (22 nm superperiod) that is a thermodynamic equilibrium phase. The superstructure formation does not depend on total surface coverage and is already observed in the initial growth stage: the superstructure size is an intensive property of the system. The triangularly shaped superlattice consists in alternating hexagonal domains resulting from the C_3 symmetry of both substrate and molecular tectons. We propose a growth mechanism in which the driving force results from a combination of maximized packing density and optimized intermolecular bonding.

The system described herein consists of the self-assembly of the molecule 2,3,6,7,10,11-hexahydroxytriphenylene (HHTP) on a well-defined Ag(111) surface and was studied by room-temperature scanning tunneling microscopy (STM) in an ultra-high vacuum (UHV) environment. The HHTP molecule is a triphenylene core functionalized by six hydroxy groups (Figure 1 a). Deposition of HHTP on Ag(111) can result in different phases, depending on substrate temperature during deposition.[24] For a temperature of about 470 K, the molecules organize on the surface in a hierarchical manner. At large scales, the formation of domain boundaries separating triangular shaped domains are observed. The regular arrangement of these domain boundaries in a hexagonal super-network leads to the creation of well-ordered mesoscopic arrays that can extend over several 100 nm (Figure 1 a,b). The observed period is 22 ± 2 nm and corresponds to a 20 molecule by 20 molecules superstructure. This lattice size is exceptionally large for a supramolecular self-assembly.

The detailed hierarchical structure of this phase is complex. One 22 nm-large triangular domain corresponds to a dense hexagonal arrangement of HHTP molecules. Individual molecules appear as triangles, the size of which corresponds to a flat lying configuration (about 1 nm). The mesh parameter of 11 ± 1 Å is aligned with the $[1\bar{1}0]$ high-symmetry direction of the silver substrate. LEED measurements confirmed the formation of a p(4×4) phase.[24] In

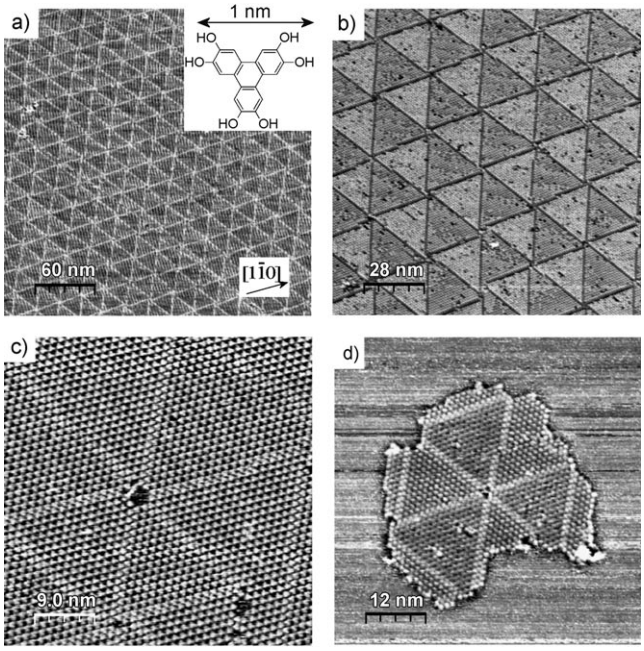

Figure 1. a,b) STM images ($U = -0.02$ V, $I = 0.4$ nA) of the supramolecular self-assembly of hexahydroxytriphenylene molecules (HHTP; inset in (a)) on Ag(111). Depending on the tip used, some molecules appear brighter, but this effect is not related to a height difference. a) 300×300 nm^2; b) 140×140 nm^2; c) 45×45 nm^2; d) 60×60 nm^2. Note the helicity at the intersection of domain boundaries (these are opposite in (b) and (c)).

[*] S. Clair, M. Abel, L. Porte
Aix-Marseille Université, IM2NP, CNRS UMR 6242
Campus de Saint-Jérôme, Case 142
13397 Marseille Cedex 20 (France)
E-mail: sylvain.clair@im2np.fr
mathieu.abel@im2np.fr
Homepage: http://www.im2np.fr/recherche/nano/Labthemat.html

[**] This work was supported by the "Agence Nationale de la Recherche" under Grant PNANO 06-0251. D. Catalin, O. Ourdjini, and R. Pawlak are acknowledged for experimental support, and F. Bocquet for helpful discussions.

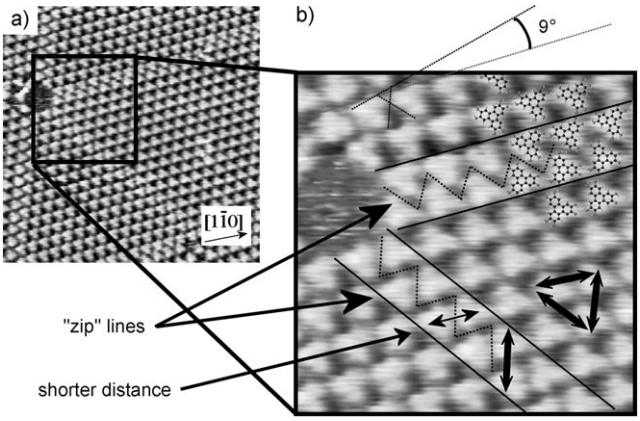

Figure 2. Details of the zip line domain boundary. a) 25×25 nm^2 STM image ($U=-0.6$ V, $I=1.5$ nA). b) Zoomed view with superimposed molecular model showing the small tilt angle in the individual orientation of the molecules with respect to the supramolecular alignment direction. Note that one intermolecular distance inside a zip line is shorter (9 ± 1 Å versus 11 ± 1 Å in the hexagonal mesh).

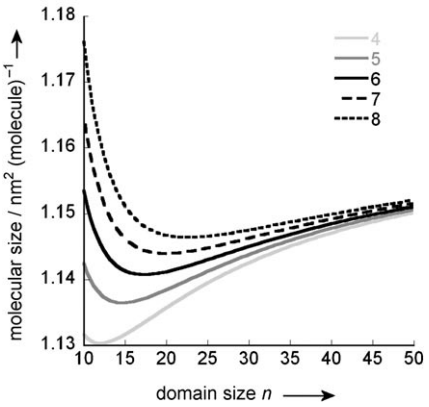

Figure 3. Average molecular size (the inverse density of molecules) as a function of domain size n calculated for different numbers of point defects (number of molecules missing at domain intersections).

neighboring domains, the molecules are individually rotated by 60°, thus forming equivalent rotational domains (Figure 2). In each domain, the baseline of each triangle representing a single molecule is not perfectly aligned with the periodicity direction but is rather slightly rotated by an angle of about 9° (Figure 2b). This minor rotation creates a domain-induced break of chiral symmetry. Remarkably, the direction of this rotation is preserved over neighboring domains so that the superstructure is enantiomerically pure. The chirality of the self-assembly can be observed in the helicity configuration at the intersection point between six rotational domains (Figure 1c). The boundary between two rotational triangular domains consists in a so-called "zip" line (Figure 2b). The molecular packing at these lines is denser and differs from the hexagonal mesh: one intermolecular distance remains unchanged (11 ± 1 Å) whereas the other is shorter (9 ± 1 Å). The positions of the molecules relative to the Ag(111) lattice thus corresponds to a (3×4) mesh along the line and to a density of one molecule per 12 silver atoms (or one HHTP per 0.87 nm^2, compared to a density of one HHTP per 1.16 nm^2 inside the domain). The intersection of six zip lines or six triangular domains is a chiral center. At such locations, molecules are systematically missing, as if the domains were not perfectly triangular but had their corners missing (Figure 1 and 2). Indeed, the higher density inside domain boundaries creates steric hinderance that prevents the formation of perfect intersections. These point defects in the supramolecular arrangement consist most of the time in the absence of one end molecule at each triangular domain corner, or six molecules at each intersection.

From the substrate registry of both domains (4×4) and zip lines (3×4), we can construct an ideal superstructure and thus derive a superlattice mesh: $((4n-1;3)\,(-3;4n+2))$ where n is the domain size or the number of molecules in the baseline of a triangular domain (with virtually no point defect). In Figure 3, we calculated the average molecular size (inverse of average density) as a function of n for an ideal superstructure where a fixed number of molecules were removed at each intersection (to account for defects). For six missing corner molecules, the densest molecular packing would be obtained with a domain size $n=17$, and the experimental value of $n=20$ would be obtained for an average 7 missing molecules.

In first approximation, the formation of the mesoscopic arrays can thus be explained by a mere optimization of the packing density of the molecular self-assembly. We shall however take also into account energetic considerations for a better description of this system. The cohesion of the self-assembly is ensured by sets of hydrogen bonds between hydroxy groups of adjacent molecules. We assigned the different bonding configurations that can occur: E_i is the bonding energy between molecules inside a domain, E_l is the energy inside a zip line (domain boundary), and E_d the energy at defect sites (for unsaturated molecules at domain corners). All energies are per dihydroxy group (Figure 4a). As the bonding between molecules occurs by formation of similar hydrogen bond types, all bonding energies must be of the same order of magnitude. In fact, the bonding energy E_i was previously estimated to be -0.15 eV,[24] and it can be expected that E_d is close to $2/3\,E_i$. We carefully counted the number of each bonding types inside a triangular domain, where exactly six molecules were removed at each intersection. We derived the total energy per unit area in function of domain size n, which indeed shows a minimum for finite n. We adjusted simultaneously the two parameters E_l and E_d to position the energy minimum at about $n=20$, as observed experimentally (Figure 4b). Intuitively, more favorable line or defect energies deliver a smaller optimum domain size. However, our model is underdetermined so that various combinations of E_l and E_d can provide reasonable experimental fit. The cases with $E_d=-1$ and with $E_d=-0.33$ are rather improbable, but the model still delivers well-positioned energy minimums, showing that the superstructure formation is intrinsic to the system and only weakly depends on energetic considerations. By considering $E_i=-0.15$ eV,[24] we can estimate $-0.16\text{ eV}<E_l<-0.14$ eV and $-0.13\text{ eV}<E_d<-0.07$ eV.

We can conclude that the actual gain in energy for a finite size superstructure amounts to 1.5–2%. Similar relatively small energy gains have already been reported as being responsible for other superstructure formations.[15,17–19] How-

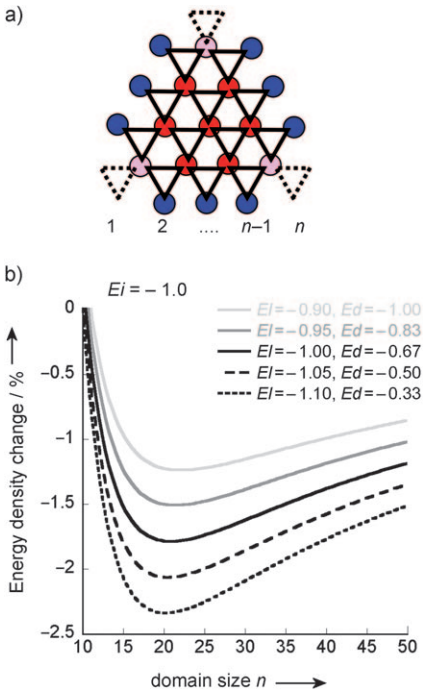

Figure 4. a) Model of the superstructure for a virtual self-assembly of domain size *n*. Red dots: bonding inside the domain (energy E_i); blue dots: bonding inside a zip line (domain boundary; energy E_l); pink dots: bonding at defect sites (energy E_d). b) Interaction energy density change by varying domain size *n* for different sets of values E_l and E_d that generate an energy minimum close to the experimental value of $n=20$ (for $E_i=-1.0$ and the reference energy set at $n\rightarrow\infty$).

ever, in those examples, the weak dependence of the total energy on the domain size allows for the coexistence of different domain sizes, which can eventually evolve depending on the total coverage. In contrast, in the case of HHTP/Ag(111), the energy minimum is well positioned and the size of the triangular structure is fixed. As a consequence, it is independent of the superdomain size and can be observed for any surface coverage. This can be clearly seen for very small domain sizes (Figure 1 d). The driving force for superdomain formation is intrinsic to the supramolecular bonding. In an atomistic view of supramolecular growth, it is more favorable to add a molecular line with the same molecule orientation as in the nucleus as long as the critical domain size is not reached. Then the formation of a zip line domain boundary is favored and the growth can continue on the next rotational domain. Furthermore, the simultaneous C_3 symmetry of both substrate and molecular tectons makes the formation of zip line intersections and thus the creation of growth nuclei highly probable.

In summary, we have described the formation of a large supramolecular template with a remarkable 22 nm period that is an intensive property of the system; that is, it does not depend on surface coverage. The driving force for this self-assembly is a combination of maximized packing density and optimized intermolecular bonding: The formation of triangular domains and zip lines domain boundaries tends to increase the packing density of the film, but this effect is retarded by the intrinsic point defects at domain intersections that are unfavorable. The equilibrium domain size involves a very high number of molecules (20×20 superstructure). We have shown previously that this system can evolve to an open nanoporous phase upon annealing.[24] Thanks to its simple design and its many hydroxy functional groups, HHTP molecules thus form a rich variety of phases upon adsorption onto a surface and are a versatile system for creating 2D supramolecular templates.

Received: June 2, 2010
Published online: September 21, 2010

Keywords: hydrogen bonds · nanostructures · scanning probe microscopy · self-assembly · supramolecular chemistry

[1] J. V. Barth, *Annu. Rev. Phys. Chem.* **2007**, *58*, 375.
[2] J. Elemans, S. B. Lei, S. De Feyter, *Angew. Chem.* **2009**, *121*, 7434; *Angew. Chem. Int. Ed.* **2009**, *48*, 7298.
[3] H. Liang, Y. He, Y. C. Ye, X. G. Xu, F. Cheng, W. Sun, X. Shao, Y. F. Wang, J. L. Li, K. Wu, *Coord. Chem. Rev.* **2009**, *253*, 2959.
[4] L. Bartels, *Nat. Chem.* **2010**, *2*, 87.
[5] R. Otero, M. Schöck, L. M. Molina, E. Lægsgaard, I. Stensgaard, B. Hammer, F. Besenbacher, *Angew. Chem.* **2005**, *117*, 2310; *Angew. Chem. Int. Ed.* **2005**, *44*, 2270.
[6] M. Lackinger, W. M. Heckl, *Langmuir* **2009**, *25*, 11307.
[7] N. Zhu, T. Osada, T. Komeda, *Surf. Sci.* **2007**, *601*, 1789.
[8] J. A. Theobald, N. S. Oxtoby, M. A. Phillips, N. R. Champness, P. H. Beton, *Nature* **2003**, *424*, 1029.
[9] S. Stepanow, M. Lingenfelder, A. Dmitriev, H. Spillmann, E. Delvigne, N. Lin, X. Deng, C. Cai, J. V. Barth, K. Kern, *Nat. Mater.* **2004**, *3*, 229.
[10] J. M. MacLeod, O. Ivasenko, C. Y. Fu, T. Taerum, F. Rosei, D. F. Perepichka, *J. Am. Chem. Soc.* **2009**, *131*, 16844.
[11] Y. Wei, S. W. Robey, J. E. Reutt-Robey, *J. Am. Chem. Soc.* **2009**, *131*, 12026.
[12] H. L. Zhang, W. Chen, H. Huang, L. Chen, A. T. S. Wee, *J. Am. Chem. Soc.* **2008**, *130*, 2720.
[13] S. Clair, S. Pons, H. Brune, K. Kern, J. V. Barth, *Angew. Chem.* **2005**, *117*, 7460; *Angew. Chem. Int. Ed.* **2005**, *44*, 7294.
[14] K. Ait-Mansour, P. Ruffieux, P. Groning, R. Fasel, O. Groning, *J. Phys. Chem. C* **2009**, *113*, 5292.
[15] Y. Y. Wei, S. W. Robey, J. E. Reutt-Robey, *J. Phys. Chem. C* **2008**, *112*, 18537.
[16] G. Schull, R. Berndt, *Phys. Rev. Lett.* **2007**, *99*, 226105.
[17] J. Zhang, B. Li, X. F. Cui, B. Wang, J. L. Yang, J. G. Hou, *J. Am. Chem. Soc.* **2009**, *131*, 5885.
[18] Y. C. Ye, W. Sun, Y. F. Wang, X. Shao, X. G. Xu, F. Cheng, J. L. Li, K. Wu, *J. Phys. Chem. C* **2007**, *111*, 10138.
[19] W. D. Xiao, X. L. Feng, P. Ruffieux, O. Groning, K. Mullen, R. Fasel, *J. Am. Chem. Soc.* **2008**, *130*, 8910.
[20] G. Pawin, K. L. Wong, K. Y. Kwon, L. Bartels, *Science* **2006**, *313*, 961.
[21] J. Weckesser, A. D. Vita, J. V. Barth, C. Cai, K. Kern, *Phys. Rev. Lett.* **2001**, *87*, 096101.
[22] A. Schiffrin, A. Riemann, W. Auwarter, Y. Pennec, A. Weber-Bargioni, D. Cvetko, A. Cossaro, A. Morgante, J. V. Barth, *Proc. Natl. Acad. Sci. USA* **2007**, *104*, 5279.
[23] J. Schnadt, E. Rauls, W. Xu, R. T. Vang, J. Knudsen, E. Laegsgaard, Z. Li, B. Hammer, F. Besenbacher, *Phys. Rev. Lett.* **2008**, *100*, 046103.
[24] R. Pawlak, S. Clair, V. Oison, M. Abel, O. Ourdjini, N. A. A. Zwaneveld, D. Gigmes, D. Bertin, L. Nony, L. Porte, *ChemPhysChem* **2009**, *10*, 1032.

